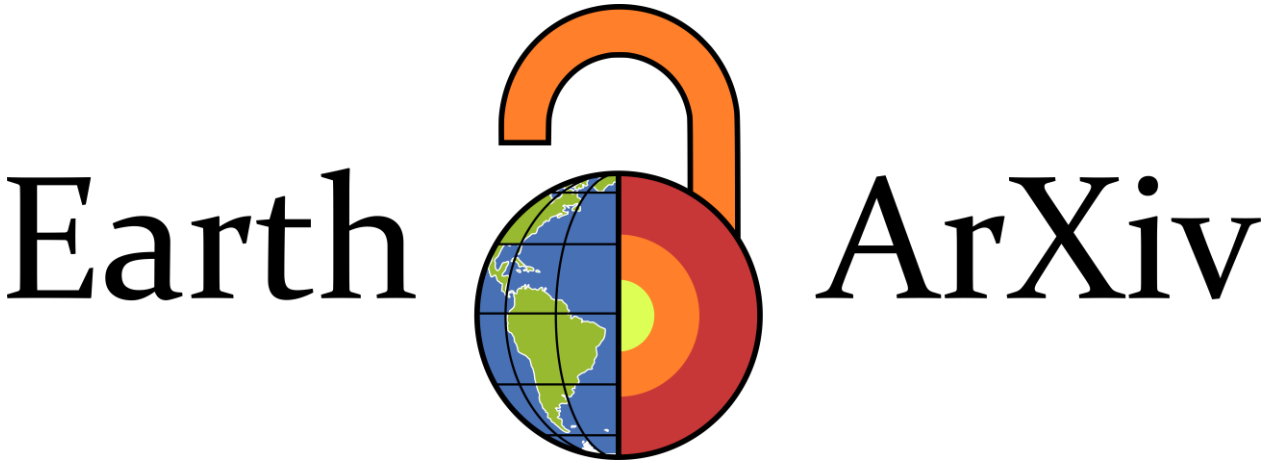

Mapping the interaction of a pyroclastic density current with irregular topography: the chemically-zoned, low aspect-ratio Green Tuff ignimbrite, Pantelleria, Italy

Rebecca Williams[1*], Mike Branney[2], Tiffany Barry[2]

1. School of Environmental and Life Sciences, University of Hull
2. School of Geography, Geology and the Environment, University of Leicester

*Rebecca.williams@hull.ac.uk

Abstract

Pyroclastic density currents are known to have high mobility, overtopping topographic barriers great distances from source. However, how density currents interact with topography is not yet fully understood, particularly with regard to dense, granular, sustained currents. We used detailed chemical mapping to show how the response of an individual pyroclastic current to topographic barriers changed with time – the current first flowing around hills, and later (during peak flow) overtopping them. The pristine, welded Green Tuff ignimbrite was deposited over irregular topography during the most recent (c. 46 ka) large explosive eruption on Pantelleria, Italy. The main (low aspect-ratio) ignimbrite flow-unit is gradationally zoned, systematically from pantellerite (base) to trachyte (top) and indicates that the composition of the pyroclastic density current gradually changed with time. Different geographic distributions of the individual compositional zones within the ignimbrite have enabled us to reconstruct a succession of snapshots of the current's evolution. The geographic 'footprint' of the current changed with time as the current gradually waxed and later waned. When the current initially encountered a hill or barrier, it was not able to overtop the hill. First it was blocked, reflected, or deflected around the lower flanks of barriers, including conical hills and transverse ridges. This is also recorded in imbricated clasts, and in rotated clasts in the more rheomorphic portions of the deposit. However, the current rapidly evolved as the eruption waxed, shifting thalwegs laterally and prograding across the island. The current progressively inundated, and then overtopped hills, during peak flow conditions. Later, as the current waned, it gradually retreated from summits, and once again became blocked or reflected by the hills. Such incrementally shifting responses of a pyroclastic density current to topography is consistent with shifting depositional patterns recorded in ignimbrites elsewhere (e.g. Poris ignimbrite, Tenerife). Such behaviour would probably be easily overlooked in ignimbrites that do not show compositional zoning but is to be expected wherever density currents are sustained and should probably be considered when assessing hazards at explosive volcanoes.

1 Introduction

Pyroclastic density currents are mixtures of pyroclasts, lithics and gas and are one of the most hazardous phenomena related to volcanic eruptions. These mixtures propagate laterally as ground-hugging gravity flows, driven by the density difference with the

atmosphere and inertia, and are influenced by topography (Aravena and Roche, 2022). Their high mobility and dynamic pressures pose a great risk to life and infrastructure. PDCs account for the deaths of >91,000 people since 1600AD (Auker et al., 2013). Improved understanding of the behaviour of PDCs would allow for better hazard and risk assessments. Traditionally, hazard maps have been based on mapping of volcanic deposits and more recently using numerical modelling and computer simulations that rely on topographic data to produce hazard maps (Ogburn et al., 2023). As such hazard assessments, particularly those using the concept of the energy cone, often delineate safe zones in the leeside of significant topographic barriers (e.g. Sheridan, 1979, Barberi *et al.* 1992, Lirer *et al.* 2001, Sheridan *et al.* 2005).

How density currents interact with topography is not yet fully understood, particularly with regard to sustained currents, and energetic currents that are not confined to within valleys (e.g. those that deposit low aspect-ratio ignimbrites). These currents are also harder to simulate numerically; popular tools such as Titan2D and VolcFlow are known to capture well the inundation area of single-pulse, valley-confined, small-volume flows but struggle to effectively simulate sustained, highly unsteady, large-volume flows, which are often partially unchannelised (Ogburn & Calder 2017). Dense, or concentrated PDCs are strongly controlled by the underlying topography, typically through channelisation which can increase their runout distance (Capra et al., 2018; Charbonnier et al., 2013; Flynn & Ramsey, 2020; Fujii & Nakada, 1999; Macorps et al., 2018; Ogburn et al., 2014; Saucedo et al., 2002; Sulpizio et al., 2010; Aravena and Roche, 2022). Valley-confined flows, however, are known to overspill and override the edges of the channel, into unconfined areas posing a significant hazard (e.g., Unzen, 1991; Merapi, 2010; Volcán de Fuego, 2018; Kubo Hutchison & Dufek, 2021; Charbonnier et al., 2023). Whilst topographic barriers are known to block currents, dilute currents are also known to be able to surmount significant topographic barriers far from source, attributed to either high momentum, a critical current thickness: height of barrier ratio, or flow stripping (; Aramaki & Ui 1966; Miller & Smith 1977, Ferriz & Mahood 1984; Wilson 1985; Fisher 1990; Fisher *et al.* 1993; Gardner *et al.* 2007; Bourdier & Abdurachman 2001; Calder *et al.* 1999; Giordano *et al.* 2002; Burgisser 2005; Gardner *et al.* 2007; Andrews & Manga, 2011). Turbidity currents can be reflected or deflected by topography (Edwards *et al.* 1994; Kneller *et al.* 1991; Pickering *et al.* 1992; Wang et al., 2025) but this is not well demonstrated to occur for PDCs in volcanic settings though has been inferred from experimental studies (Bursik & Woods 2000; Woods *et al.* 1998).

1.1 The Green Tuff Formation, Pantelleria

The island of Pantelleria is located in the Strait of Sicily and lies approximately 70 km east of the coast of Tunisia. The 45.7 ± 1.0 ka Green Tuff Formation is the youngest product of an ignimbrite-forming eruption on Pantelleria (Jordan et al., 2018; Rotolo et al., 2021) and is chemically zoned from pantellerite (SiO_2 = 70 wt %) to trachyte (SiO_2 = 62 wt %) (Fig. 2; Mahood et al., 1986, Williams, 2010; Williams et al., 2014). The matrix varies from vitrophyric (e.g. at top and base) to lithoidal. Much of the Green was probably deposited in the sea, with the onland volume estimated as 0.28 km^3 (Jordan et al., 2018). The Green Tuff ignimbrite (AR <1:3125), has been chosen as a case study as it is superbly exposed both

longitudinally from source as well as laterally around the island (Fig. 1).

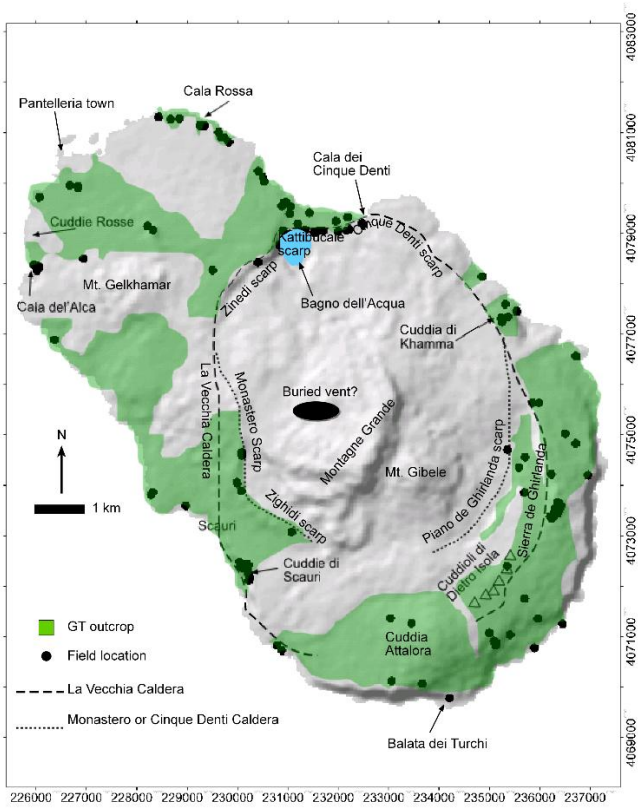

Figure 1: A location map of Pantelleria, Italy. Extent of the Green Tuff (GT) outcrop is marked in green.

Williams, 2010 defined the Green Tuff Formation (new term) as a palaeosoil-bound peralkaline eruption-unit which covered the entire island of Pantelleria based upon a lithofacies approach, summarized in Figure 2 (full description of the lithofacies is provided in the supplementary material). It comprises a loose pumice-lapilli layer, the Kattibucale Member (new term) interpreted as a pumice fall deposit, which is defined at the Monastero scarp (Fig. 1). This is overlain by a variably stratified, eutaxitic lapilli-tuff with local lithic breccia lenses and is intensely rheomorphic in parts. This Member is named the Green Tuff ignimbrite (defined at the Kattibucale scarp, Fig. 1) and it reaches thicknesses of over 20 m in palaeovalleys, but thins to less than 1 m on topographic highs and steep slopes. It is interpreted to be the deposit from a single, sustained, quasi-steady pyroclastic density current.. Where strongly rheomorphic, ductile extension and intense folding is observed and is interpreted to have occurred predominantly during deposition (Branney et al. 2004; Catalano, S. G. et al. 2007; Williams et al. 2014, Rotolo et al., 2021; Scarani et al., 2023). The strong welding has been attributed to its peralkaline chemistry, high magmatic temperature of 930- 960°C and volatile resorbtion (Scarani et al., 2023). The low-viscosity of the pyroclasts and their agglutination style of deposition mean that deposits smeared the entire landscape, including slopes up to 90° (Catalano et al. 2007). Usefully this means it is unlikely that the current was able to bypass anywhere without it leaving behind evidence of its passing. Although the Formation is often strongly welded, primary characteristics can be observed such as lithic lenses, crystal rich layers, vitroclastic textures, and pumice concentration zones, even when rheomorphic.

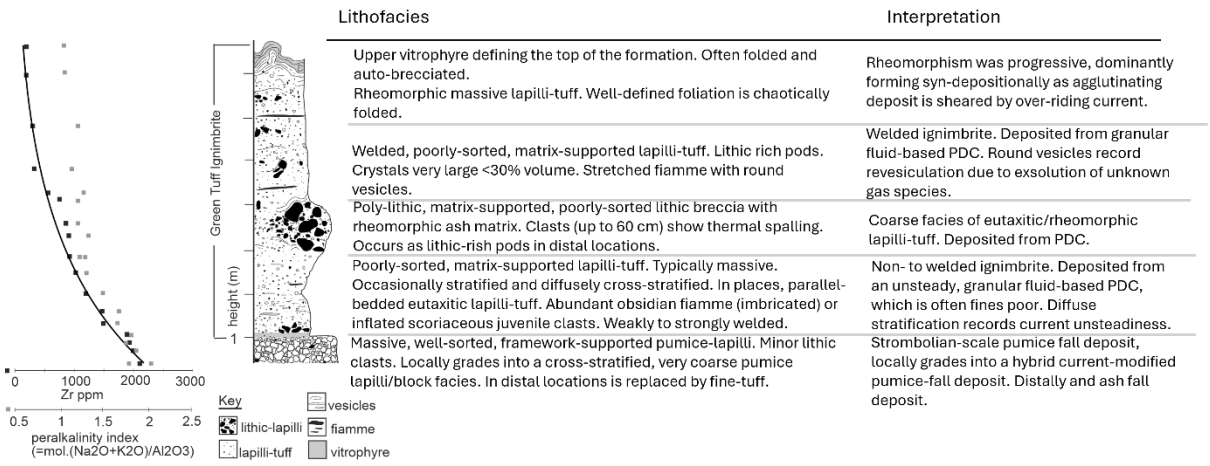

Figure 2: Generalised vertical stratigraphy of the Green Tuff Formation showing vertical geochemical trend in zirconium (Zr) and peralkalinity index. Summary lithofacies descriptions and interpretations given; for full details, see supplementary material S2.

Here we summarise the eruption history of the Green Tuff Formation following Williams, 2010 and Williams et al., 2014 (Fig. 2). The eruption of the Green Tuff Formation began with a sub-plinian eruption column. This emplaced a local pumice-lapilli deposit and more distally, an ash deposit. As the eruption waxed, introducing larger pumice and lithic clasts into the plume, the column was no longer able to remain fully buoyant. Turbulent near-vent currents or eddies deposited hybrid fall and current deposits along caldera scarps. The eruption style rapidly evolved into low-fountaining, producing a quasi-steady, sustained pyroclastic density current. This current was initially a high-concentration, granular fluid-based current, but experienced periods of turbulence. As the eruption sourced hotter particles, the current unsteadiness remained and the flow boundary zone was transitional between granular flow-dominated and fluid-escape dominated flow regimes. The hot, sticky particles welded instantly upon deposition. As the eruption further waxed, the current exerted intense shear on the aggrading agglutinate, deforming the deposit. As the deposit continued to aggrade, the zone of shear migrated upwards. Progressive evacuation of the magma chamber brought up magma that was more crystal rich, possibly from deeper depths within the chamber. The onset of the climactic phase is marked by a lithic breccia deposited in the west of the island. The eruption caused fragmentation or erosion of the conduit walls or the roof of the magma chamber. Partial caldera-collapse may have occurred at this stage. The pyroclastic density current continued, becoming more widespread, depositing upon the entire island. The current travelled up to 45 km along the seabed, initiating volcaniclastic turbidites which travelled even further (Anastasakis & Pe-Piper 2006). Shear intensity increased, causing dramatic rheomorphism of the aggrading Green Tuff deposit. The eruption ended with the pyroclastic density current, which covered the entire island in a hot, glassy deposit sterilizing over 100 km2 of land and an unknown area of the sea floor. The uppermost horizon of the deposit, folded dramatically by the final phase of the current, chilled against the air and autobrecciated. As the deposit cooled, further rheomorphism occurred as the deposit crept down slopes and pockets of hot melt oozed before chilling rapidly. After the Green Tuff eruption, effusive activity resumed immediately, with the eruption of the Mounte Gibele trachyte lava shield (Mahood & Hildreth 1986). The top of the Green Tuff ignimbrite is commonly eroded when not covered by younger deposits. It is also often stripped for use as a building material. There is no evidence of a well-developed soil.

The objective of this study is to use the field relations of the internal chemical stratigraphy of the Green Tuff ignimbrite two investigate two elements of this history in detail: (1) how do

sustained PDCs interact with different shapes of topography: and (2) does the Green Tuff formation record a caldera-forming eruption?

1.2 Entrachrons and their use in reconstructing ignimbrite emplacement

A conceptual line or surface that joins the first appearance of pyroclasts in the deposit is a form of time-marker through that deposit and has been termed an 'entrainment isochron' or 'entrachron' (Branney & Kokelaar 2002). An entrachron may be represented by the first appearance of a distinct composition of pumice, crystal or lithic clast (Branney & Kokelaar 1997) and need not be related to a break in deposition (i.e. disconformity). An ignimbrite that has a gradational chemical zoning pattern may be described as containing a continuous series of entrachrons as the chemistry changed (e.g. appearance of SiO2 > χ weight %), enabling detailed assessment of its internal architecture.

The Green Tuff Formation is laterally variable and lithofacies are not spatially extensive and are here not used as a basis for a lithostratigraphy. Previous studies have used geochemical correlation techniques to assess the emplacement of a compound ignimbrite where the deposit formed by incremental emplacement of packages from distinct flows (e.g. Valley of Ten Thousand Smokes, Fierstein & Wilson 2005). The Green Tuff is compositionally zoned, and is defined at a type section (Fig. 2 Williams, 2010; Williams et al., 2014). Mapping of this novel chemical-entrachron has been previously applied to map the temporal evolution of the Green Tuff PDC, revealing a waxing and waning flow front (Williams et al., 2014). Here, we apply the Zr-entrachron to interrogate the internal architecture of the ignimbrite over irregular topography.

2 Methods

2.1 Mapping and Logging

The Green Tuff Formation was mapped and logged in detail to document the lateral, vertical and longitudinal variations of the ignimbrite. Lithofacies descriptions are given in the supplementary materials. Locations where the Green Tuff is well exposed up and around topography were chosen for individual study (Fig. 1). The Green Tuff ignimbrite was logged and sampled across each topographic barrier. Vertical sections were selected for sampling at localities where the base of the ignimbrite unit was exposed, to ensure that the very first part of the current was recorded. Whilst care was also taken to sample the very top of the ignimbrite, some erosion of the uppermost parts of the ignimbrite is common. In sites that do not preserve an upper vitrophyre, we cannot be certain whether the top of the unit is present. Each case-study was mapped in the field onto an enlarged 1:25,000 topographic map (Instituto Geografico Militare, Edizione 2, 1972).

2.2 Kinematic indicators

The dip and strike of the contact of the Green Tuff with the substrate were taken as the slope of the pre-Green Tuff surface. Bedding and eutaxitic foliation of the Green Tuff ignimbrite were measured where not modified by rheomorphic folds. The plunge direction of imbricated fiamme and clasts is anti-parallel to the transport direction of depositing parts of the current. For example, an imbrication of 10/090 with respect to horizontal bedding indicates an inferred current direction from east to west (Schmincke & Swanson 1967; Branney & Kokelaar 1992). Imbricated clasts are mapped as arrows pointing in the inferred current direction (i.e. 180° to plunge direction). The plunge and plunge direction of lineations on bedding or eutaxitic foliation planes give an indication of rheomorphic shear direction at the base of the current in the final stages of agglutination (Schmincke & Swanson 1967; Andrews & Branney 2011). Shear may be the result of the overriding current (Branney & Kokelaar 1992; Andrews & Branney 2011), or due to gravity acting on the hot agglutinate on a local topographic slope. Orientated samples were collected at some localities for thin

section analysis, allowing for micro-kinematic analysis (e.g. σ - and δ -type objects). Here, directional (kinematic) data are recorded in conjunction with a chemical-entrachron stratigraphy so that, uniquely, the inferred emplacement of the density current has temporal control.

2.3 Geochemistry

Over 400 samples were collected from over 80 vertical sections through the Green Tuff Formation around the island (Fig. 1) for whole rock X-ray fluorescence spectrometry analysis (XRF). A subset of these samples from the type section (Williams et al., 2014) were also analysed by laser ablation-inductively coupled plasma mass spectrometry (LA-ICP-MS). Details of each of the analytical methods and full datasets are given in Supplementary Materials. A wide range of elements show a linear trend through the deposit such as Y and Nd, but Zr shows the widest range spanning over 1400 ppm (Fig. 2). The decrease in Zr from >2000 ppm at the base of the deposit to < 800 ppm at the top tracks the evolutionary trend from pantellerite to trachyte (Williams 2010). Zirconium is immobile and resistant to post-depositional weathering, therefore closely reflects the original composition of the erupted magma. On this basis we use the Zr concentrations to define a chemical stratigraphy for the Green Tuff ignimbrite. Deposits of high Zr ppm were erupted at the start of the eruption with systematically decreasing Zr concentrations erupted with time through the eruption (Williams et al., 2014).

To determine the distribution of Zr values across the island values were entered into a GIS database (ArcMap 9.2; ESRI inc.) with the x,y coordinates of their location overlying topographic data (A 30 m resolution ASTER digital elevation model; https://lpdaac.usgs.gov/Acquisition Date: 2002/08/15 Path: 190 Row: 34). Each point in the database has a geographical co-ordinate and a Zr ppm value. The database can be queried to show the spatial distribution of a particular Zr ppm value.

For simplicity the gradational variations of Zr ppm through the Green Tuff ignimbrite were divided into eight zones to enable clear analysis of the distribution of Zr values through the deposit: the pantelleritic end member (>2000 ppm), the trachytic end member (<800 ppm), and intervals of 200 ppm through the gradational member (t1-8). Each zone was queried in GIS and isometric areas derived, i.e. areas were drawn around locations with the same Zr range. These isometric areas are interpreted to represent a brief time span of the ‘footprint’ of the depositing PDC within the duration of the eruption (Williams et al. 2014). The boundaries of the zones are intergradational and are equivalent to chemically defined entrachrons. Therefore, studying these footprints successively from high Zr ($t_{1;}$ early) to low Zr ($t_{8;}$ late) enables us to track how the current changed with time, and how it interacted with the topography. At case study localities, the vertical chemical stratigraphy was logged systematically across topographic features in conjunction with lithofacies analysis and kinematic indicators.

3 Results

The Green Tuff ignimbrite drapes a variety of topographic features including caldera scarps, old scoria cones and pumice cones, as well as infilling palaeovalleys which are extremely well exposed along the coast. A variety of different case studies have been investigated: conical barriers of three different sizes (Cala dell’Alca scoria cone, Cuddia di Khamma and Cuddia di Scauri), ridges perpendicular to the current direction (Piano and Serra di Ghirlanda) and two palaeovalleys parallel to palaeocurrent direction (Cala Rossa and Balata dei Turchi) (Fig 1). Localities along the proposed caldera walls were also investigated to determine the timing and extent of caldera collapse during the Green Tuff eruption.

Minimum velocities for currents can be estimated from their run-up heights at topographic barriers (Wilson & Walker 1981; Legros & Kelfoun 2000; Brand & Clarke 2012) using a simplified version of the Bernoulli equation, assuming that the pressure and density of the currents does not change from the bottom to the top of the barrier:

$$U = \sqrt{2gH} \quad (1)$$

Where U is velocity, g is the acceleration due to gravity and H is the relative height of the topographic barrier. Using this equation, it is possible to estimate the maximum velocity for the current when blocked by different topographic barriers, and conversely, a minimum velocity when the current was able to pass over the barrier. However, this velocity calculation is only valid as long as the flow depth is small compared to the obstacle height. Other factors not considered by this equation are mass flux and momentum. The velocities of the current at different stages of the eruption are calculated for each of the topography case studies.

3.1 Interaction with small hills

3.1.1 Scoria cone at Cala dell'Alca

A small (c.15 m high) scoria cone is draped entirely by the Green Tuff ignimbrite on the northwest coast of Pantelleria (Fig. 1; Fig. 3a). A current direction from the SE, inferred from SE-NW trending rheomorphic lineations, is consistent with a source vent near the centre of the island (Fig. S3.1). However, on the scoria cone flanks, current kinematic indicators appear to be strongly affected by the slope: both lineations and imbricated clasts show down slope flow (Fig. 3c). Imbricated fiamme and lineations on the stoss-slope suggest both SE and NW flow directions.

The entrachron stratigraphy in the Green Tuff ignimbrite changes across the cone. In particular, the base of the ignimbrite is demonstrably diachronous (Fig. 3b). The first zone (t1) of the ignimbrite is absent in this part of the island. The next zone of the current (t2) only drapes the eastern flank of the cone and zone t3 is only recorded on the eastern side of the summit. Zone t4 is present across the entire zone including the lee side of the cone. All subsequent chemical entrachrons (t5-7) are present on the lee side of the barrier. The western draping section has an upper vitrophyre, suggesting that the ignimbrite is complete here. The final zone (t8) is absent.

Interpretation

The first phase of the current (t1) did not reach this part of the island. The leading edge of the current advanced with time, reaching the cone by t2, but was unable to surmount it. Using equation 1, the maximum velocity for this stage of the current was ~17 ms−1. The next phase of the current, t3, was able to inundate the cone further but it is not until time-slice t4 that the current is able to pass over the barrier completely, presumably at velocities in excess of 17 ms-1. The current continues to flow over the barrier, but the leading-edge retreats during t7 and the final phase of the current t8 did not reach here. Imbricated fiamme near the base of the deposit point back towards the current source and are interpreted to show that at the flow-boundary layer, the depositing current was actually travelling back in the direction of the general current direction (Fig. 3c) suggesting that the current, at this stage, was reflected by the cone. An alternative interpretation is that this kinematic indicator records post-depositional, downslope modification (e.g. Wolff & Wright 1981). However, the lack of rheomorphic folding or extensional features at this location does not support this.

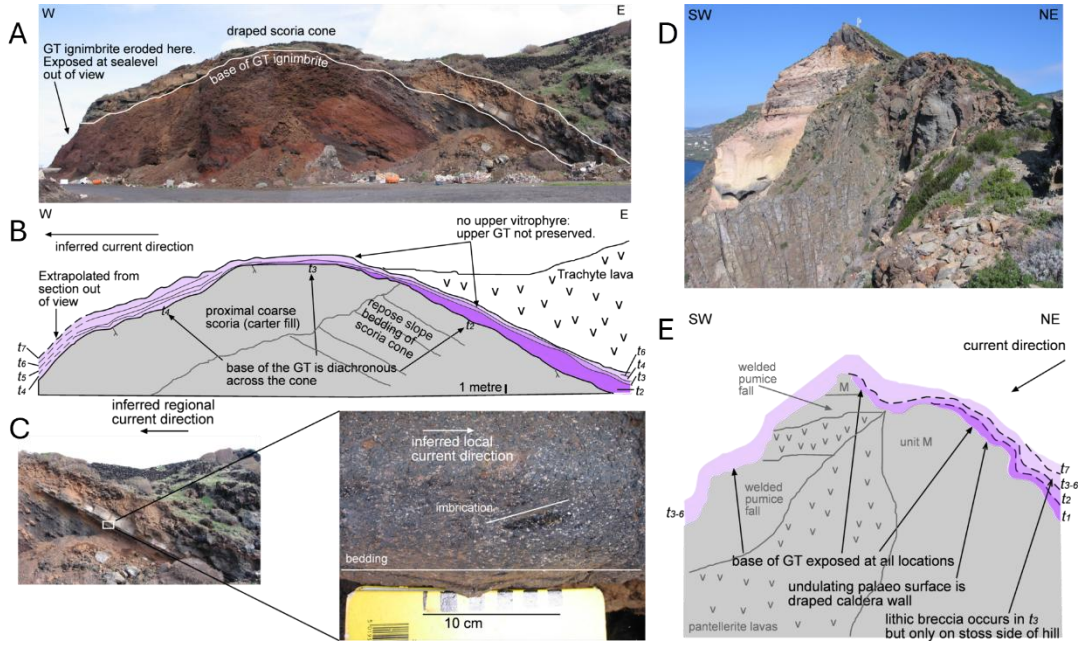

Figure 3: The interaction of the Green Tuff with small hills. The GT drapes Cala dell'Alca (A), with a diachronous base as picked out by the Zr zones (B). Imbricated fiamme suggest reflection of the current in the initial stages (C). The GT drapes Cuddia di Scauri (D) with a diachronous base as picked out by the Zr zones (E).

3.1.2 Cuddia di Scauri

An eroded pumice cone, Cuddia di Scauri rises above the surrounding topography by c. 30 m to along the La Vecchia caldera scarp near Scauri (Fig. 1, Fig. S3.2). The Green Tuff ignimbrite drapes this cone but is mostly thin (<1 m). The base is always exposed and dips from 20° to 80° (Fig. 3d).

The inferred general current direction of the Green Tuff PDC away from its vent is towards the southwest, however, palaeocurrent indicators show a range of orientations (Fig. S3.2). On stoss flanks of the cone, lineation trends vary from southeast to northeast. At the summit of the pumice cone, imbricated fiamme indicate a palaeocurrent direction to the southwest and lineations trend to the west on lee flanks. On the proximal south flanks of the cone lineations trend east-west, perpendicular to the north-south trending scarp. Rotated clasts indicate upslope, westward current direction. Further south however, imbricated clasts indicate palaeocurrent direction to the south, downhill from the pumice cone (Fig. S3.2) or towards the southeast.

All locations logged and sampled at Cuddia di Scauri have the Green Tuff exposed to the base (Fig. 3d). The first zone of the ignimbrite (t1) is only recorded on the stoss side of Cuddia di Scauri. Through zone t2, the footprint of the ignimbrite increases on the northern flanks of the cone. During the following four zones (t3-6), the ignimbrite is recorded across the entire area (Fig. 3e). The final zone recorded at Cuddia di Scauri is t7, and this is restricted to the stoss and northern flanks of the cone. Successive divisions in the chemical-entrachron stratigraphy overlap underlying zones, showing that the base of the unit is diachronous across the topographic barrier.

Interpretation

The very first phase of the current reached this area but was only able to inundate the flatter areas around the cone. It also appears to be constrained by the caldera scarp which runs parallel to the coastline. During t2, the current began to advance up the lower northern flanks

of the cone. To the north of the cone, at its base, lineations and imbricated fiamme suggest a north westerly current direction which swings round to a more westerly direction further away from the cone. This may indicate that the current was being deflected here around the northern flanks of the cone.

The current then surmounted the entire cone and continued this inundation during t3-6. At the very top of the cone the predominant flow direction remained towards the SE, straight across the cone, with no deflection from the regional current direction. However, during the early phases of this stage the lineation and imbricated fiamme data on the southern flanks indicate flow to the south, and to the southeast. This suggests that the basal parts of the current during deposition are affected by the palaeotopography and the current was deflected and reflected by the caldera scarp. During t7, the final (waning) stages of the current, it does not overtop the summit of the cone but rather flowed around its northern flanks and was constrained once again by the caldera scarp.

The phase of the current which overtops the barrier is associated with a lithic breccia which occurs on the south side of the barrier. This suggests that this phase (t3-t6) of the current was peak flow and may represent a climactic phase of the eruption, with minimum velocities of 25 ms^{-1} (equation 1).

3.1.3 Cuddia di Khamma

A similar record of events is also seen at Cuddia di Khamma, a lava shield volcano in the east of the island (208 m a.s.l, differential height c. 30 m). Here, only the t6 phase of the current was able to over top the hill, suggesting that up until then the current velocity had been <25 ms^{-1}, and in excess of this as the current passed over.

3.2 Interaction with transverse ridges

3.2.1 Piano & Serra di Ghirlanda

Two sub-parallel, circumferential ridges occur on the south of the island (Fig.1). Piano di Ghirlanda, the inboard ridge, is thought to be part of the Cinque Denti caldera and the outermost Serra di Ghirlanda ridge, which rises 184 m above the plain between it and Piano di Ghirlanda to 384 m a.s.l. Serra di Ghirlanda is thought to be the rim of an older caldera named La Vecchia (Mahood & Hildreth 1986). The Green Tuff ignimbrite is cut by the inner Piano di Ghirlanda scarp which indicates that some movement along this fault occurred during or after the eruption of the Green Tuff. A line of pumice cones, named the Cuddioli di Dietro Isola continues the trend of the outermost ridge where its topographic trace becomes buried underneath the Cuddia Attalora shield volcano (560 m a.s.l, 135 m differential height) that post-dates this scarp (Fig. 1).

The Green Tuff drapes the Serra di Ghirlanda scarp and the plains to the stoss and lee side of it (Fig. S3.3). Basal exposures are limited to a handful of localities as are good exposures of lineations and foliations, thus there are limitations to the detail of interpretations here. Good sections through the Green Tuff ignimbrite occur along the coast exposing both the lower contact and upper vitrophyres. On Serra di Ghirlanda, most lineations trend perpendicular to the ridge axis. At the southern end of the ridge, some trend SSE which is down slope in this area, suggesting the influence of the underlying topography (Fig. S3.3).

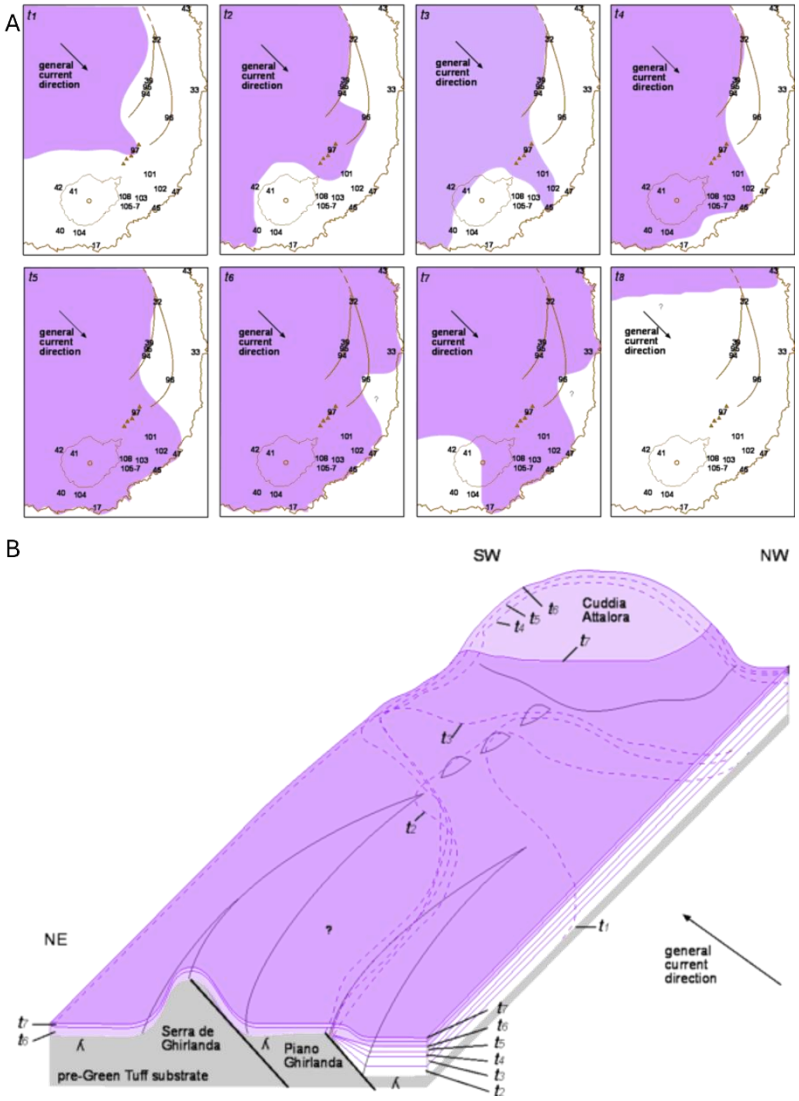

Figure 4: A: Geochemical footprints of the density current at different time-slices through the evolution of the current from start (t1) to finish (t8) based upon Zr ppm. The two caldera scarps, Cuddia Attalora shield volcano, the line of small cones and the locations sampled for geochemical analysis are marked. B: Schematic block diagram showing change of entrachron stratigraphy over the topographic barriers. Dashed lines indicate limits of buried entrachrons.

Detailed geochemical footprints are constructed for the south of the island (Fig. 4a). The first zones of the ignimbrite (t1-2) are recorded on the stoss sides of Piano di Ghirlanda, Cuddioli di Dietro Isola and Cuddia Attalora. The next three zones (t3-5) show increasingly large footprints. Zone t6 is the only zone to be recorded over the entire area. The following zone (t7) is recorded across the two scarps and along large sections of the coast; however, it is absent from the western flank of the Cuddia Attalora shield volcano. The final chemical zone (t8) is only recorded in a narrow strip in the north of the area at Cala di Levante and is absent from the transverse scarps and Cuddia Attalora shield volcano.

Interpretation

The current distribution was strongly influenced by topography in the southern half of the island (Fig. 4b). At the very start of deposition from the current (t1) the leading edge was finger like and restricted to a topographic low between the two caldera scarps and Cuddia Attalora shield. The leading edge of the current progressively advanced towards the sea,

encroached on the Piano di Ghirlanda scarp and the deposit footprint broadened (t2). As the current waxed further (t3), its leading edge advanced over the low-lying plain between the two ridges and a narrow finger of current reached the sea. The current also began to advance over the Cuddia Attalora shield volcano, although lineations here suggest that the current was initially deflected around its lower flanks until the hill became entirely inundated. The leading edge of the current then advanced down its lee side towards the sea (t4). Velocities at this stage would have to have been in excess of 51 ms-1 (equation 1) to overtop Cuddia Attalora.

The current continued to extend further and entered the sea in all areas south and west of the Serra di Ghirlanda scarp but did not overtop this significant barrier (t5). During the next, climactic phase (t6) the current inundated the entire landscape, overtopping all topographic barriers including Serra di Ghirlanda and entered the sea along all the coastline, with a calculated minimum velocity of 60 ms^{-1} (equation 1). The current then started to wane, and no longer inundated the entire Cuddia Attalora shield volcano. Instead, it was deflected around its eastern flanks (t7). In its final phase (t8) the leading edge of the current retreated leaving just a narrow eastward-trending finger.

3.3 Interaction with palaeovalleys

The Green Tuff ignimbrite partially filled palaeovalleys and the coast provides excellent cross-section exposure through these although near-vertical cliffs make many inaccessible. Here we present two case studies: Cala Rossa and Balata dei Turchi. Where the Green Tuff ignimbrite is thick within a valley, it is here termed ‘valley fill’, where the ignimbrite is thin over an adjacent topographic high, it is here termed a veneer deposit; however, in this work these terms are used as intergradational descriptive terms without any genetic connotations (c.f. Wilson & Walker 1982).

3.3.1 Cala Rossa

At Cala Rossa (Fig 1; UTM 32s 0764785, 4081013), a small palaeovalley is exposed on the coast (Fig. 5). In the valley bottom, the ignimbrite is 6 m this compared to 1 m thick on the valley sides. Samples were analyzed from the vitrophyric base and top, and a middle sample was obtained 1.1 m above the base of the unit. A vertical cliff prohibited further sample collection. The 1m thick valley side deposit records two chemical-entrachon zones (t2 and t5) and the 6 m thick valley fill deposit records three (t2, t5, t6). The thickness of zone t2 is roughly the same across the palaeovalley (Fig. 5).

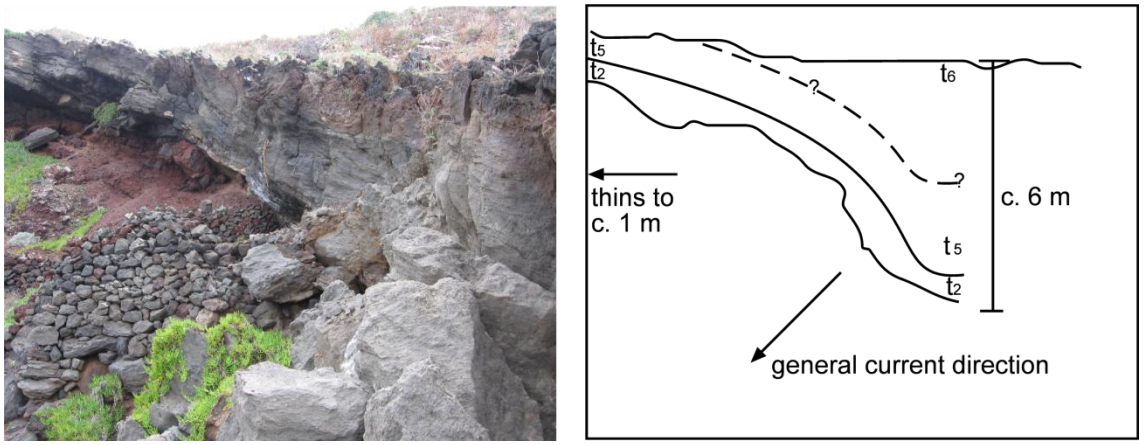

Fig 5: A: Photograph of Cala Rossa (UTM 32s, 0764785, 4081013). Note how the Green Tuff is thick in the valley bottom to the right and thins over a small topographic high to the left. B: Schematic cross-section of the unit showing entrachron stratigraphy.

Interpretation

At this site, the veneer deposit does not represent a condensed sequence equivalent to the entire valley fill succession. Rather, it was deposited at the same time as the lowest metre of the valley-fill ignimbrite. As the interfluve preserves an upper vitrophyre and is not missing any eroded succession, we can infer that the valley fill therefore continued to aggrade after deposition had ceased on the valley sides. Thus, during t6, the current in this area was valley confined, despite this time-slice appearing to be the climactic stage of the eruption. This indicates that the current was not flowing equally across the island and here may have already begun to wane.

3.3.2 Balata dei Turchi

A well exposed palaeovalley at Balata dei Turchi (Fig. 1; UTM 33s 0234198, 4069857) in the south of the island is partly filled by the Green Tuff ignimbrite. The Green Tuff Formation is up to 15 m thick in the valley fill and thins to less than a metre on the valley side. Here, both the valley fill and the veneer were emplaced during the same time-slice, suggesting that the current was not valley confined. Moreover, the current deposited on interfluve areas simultaneously with deposition in the valley axis, but the rate of deposition on the interfluves must have been lower.

Across all palaeovalleys, valley-fill and veneer lithofacies are similar, and both indicative of a granular fluid-based PDC. There is no evidence of a dilute flow boundary zone recorded on valley sides.

3.4 Interaction with caldera walls.

The Green Tuff drapes a number of scarps interpreted to be caldera walls—the Khattibucale scarp (Fig 6), the Zinedi scarp (Fig 7) and the Cinque Denti scarp. Lowermost, unwelded parts of the Green Tuff ignimbrite are observed on caldera rim sections and the upper, welded and rheomorphic parts (which outside the scarp conformably lie on the lower parts) drape and dip into the caldera (Fig 6b, 7b), and belong to the t2 entrachron zone. Unwelded, lower portions are not observed on intra-caldera slopes. The sedimentary structures, such as imbricated fiamme, show northerly palaeocurrent direction (away from the caldera) but some rheomorphic folding shows minor movement southwards, into the caldera (Fig 6b, 7b).

Six orientated thin sections were made from samples taken from 5 locations along the Zinedi (Fig 6c-h) and Kattibucale scarps (Fig 7c) where t2 Green Tuff drapes to the base of the exposed slopes. All samples contained kinematic indicators that gave a sense of shear in opposing directions. The predominant shear direction for most of the samples was upslope.

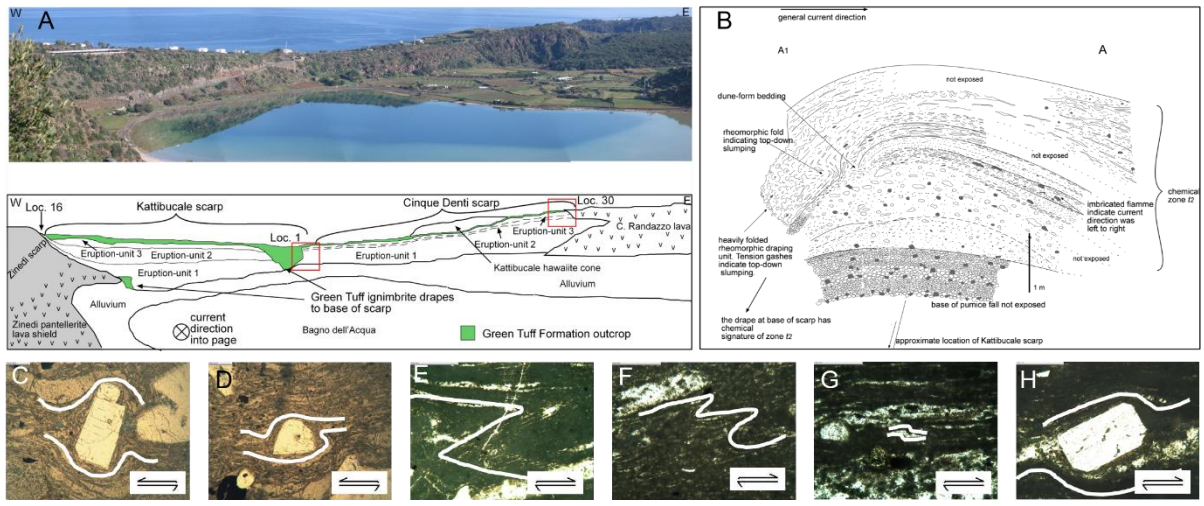

Figure 5: A: View of the Kattibucale scarp and Cinque Denti scarp looking north. The Green Tuff ignimbrite outcrops along the top of these scarps and to the base at some locations. B: Field sketch of longitudinal cross-section through the Green Tuff ignimbrite (top not shown) at the summit of Katibucale scarp (location 1). Imbricated fiamme indicate paleocurrent direction was left to right, northwards, away from the caldera. The scarp is transverse to this. Basal, non-welded parts of the ignimbrite shows diffuse bedding and overlies the basal pumice fall deposit. Outboard of the scarp (right), the lower part of the Green Tuff ignimbrite is bedded parallel to the underlying slope. At approximately 2 m above the base, the rheomorphic facies drapes the stoss (left) side of the caldera scarp. This horizon traces to the base of the scarp, 15 m below at this location and up to 50 m at others, and is chemical zone t_2. Rheomorphic folding at the top break of slope suggests minor rheomorphic downslope slumping. This indicates that up to 50 m of the scarp was extant at the time of early (t_2) stages of the Green Tuff ignimbrite. C (δ-object) and D (δ-object) are from location 16. E (verging fold), and F (verging fold) are from location 30. G (verging folds) and H (δ-object) are from location 1. Classification and interpretation of δ and σ–objects following Passchier & Simpson (1986).

Interpretation

Macro and micro kinematic indicators record both primary shear during deposition from the current as it travelled up an existing caldera wall and downslope shear, interpreted to record secondary rheomorphism as the deposit slumped downhill. At Cinque Denti, the entire Green Tuff ignimbrite traces to the base of the exposed scarp (c. 20 m). The Green Tuff ignimbrite here is of zone t_2, which was emplaced near to the beginning of the eruption. On the Zinedi scarp, the lower horizons (t_2) of the Green Tuff ignimbrite and its basal pumice fall are flat-lying, conformable with the unit below (Fig. 7b). The upper, rheomorphic horizon (t_2) drapes over these lower units to lie on progressively older ignimbrites (Fig. 7b) and is found at the base of this c.200 m scarp. This suggests that the caldera walls existed prior to the emplacement of the t2 zone of the ignimbrite, which was formed near to the beginning of the eruption.

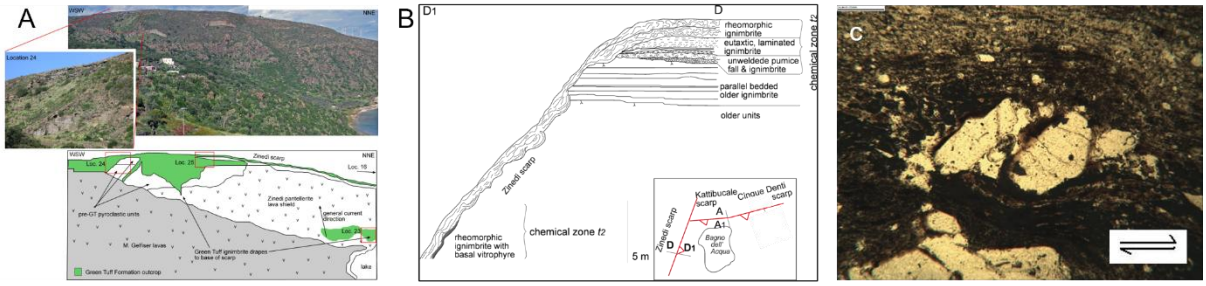

Figure 7: A: View of the Zinedi scarp looking NNW. The Green Tuff ignimbrite outcrops along the top of this scarp and to the base at some locations. Location of cross-section sketch (B) and sample for kinematic indicators shown in red box. B: Sketch of the Zinedi scarp viewed SW at location 24. The lower half of the Green Tuff ignimbrite lies conformably with the underlying units (right). The upper, rheomorphic unit of the Green Tuff drapes down c.20 m at this location (left), and to the base of the c. 200 m high scarp to the lake at location 23 (C), which is in chemical zone t2. This indicates that at least 200 m of this scarp was extant at the time of early (t2) stages of the Green Tuff ignimbrite. C: Imbricated crystals from location 23.

4 Discussion

4.1 Blocking, deflection and reflection of a dense, granular current

A range of topographic barriers have been studied from small, conical barriers to large ridges. At each location, the entrachron stratigraphy shows onlap which indicates that the base of the Green Tuff is diachronous across the barrier. Without analyzing the entrachron stratigraphy, this diachronicity would not be apparent in the field. Schematic cross sections show that the current progressively advanced over each barrier. The initial phases of the current (t1-2) are not recorded on the lee sides of any of the studied barriers suggesting that the current did not overtop the barriers at this stage. Experiments on turbulent flows suggest that currents are blocked by topographic barriers with heights greater than 1.5 times the thickness of the current (Andrews & Manga 2011). Therefore, the Green Tuff PDC was likely to be thin, not inflated and sluggish with a low velocity of up to 25 ms^{-1}. As the current waxed (t3), it was able to rise up the stoss slope (e.g. at Cala dell'Alca and Serra di Ghirlanda) and overtopped Cuddia di Scauri, which is located nearer to the inferred vent location. During the climactic phases of the current (t4-6), the current passed over all the barriers, with velocities likely in excess of 60 ms^{-1}. In the final phases of the current (t7-8) the leading edge of the current retreated and no longer overtopped the barriers.

The current was blocked in its initial phases by all the topographic barriers studied. At some locations (e.g. Cuddia di Scauri, Cuddia Attalora) the chemical-entrachrons wrap around the lower flanks of the topographic features. Directional indicators on the stoss sides of topographic barriers show that flow was either moving down slope back towards the current source (e.g. Cala dell'Alca), around barriers (e.g. Cuddia di Scauri) or along barriers (e.g. caldera scarp at Cuddia di Scauri). This suggests that at least the lower parts of the current, during the early phases of the eruption, were either reflected or deflected by the topography, a behavior previously demonstrated in turbidity currents (e.g. Kneller et al. 1991; Wang et al., 2025).

Lithofacies analysis (supplementary material 2) suggests that the Green Tuff Ignimbrite was predominantly formed from a high-concentration (i.e. dense) granular fluid-based flow-boundary zone. The thickness of this dense zone is unknown. Flow-stripping of the upper, dilute portions of a current is one hypothesis for how a PDC might overtop significant barriers. However, there is no evidence from the lithofacies analysis for deposition from a dilute current on the lee side of topographic barriers. Furthermore, there is not a systematic lack of a lithic breccia on the lee slopes of topographic barriers. As dense, granular currents have greater capacity to carry large lithic blocks than dilute currents (e.g. Roche et al., 2016), we rule out flow-stripping as a mechanism for surmounting topography.

4.2 Rapidly evolving currents and shifting thalwegs

The model originally conceived for low-aspect ratio ignimbrites, such as Taupo (Wilson & Walker 1981; Wilson 1985), is that the ignimbrite was emplaced through rapid radial flow, in which the initial current velocity was very high so that the current rapidly surmounted topographic hills to its distal limit. Chemical mapping of the internal architecture of the Green Tuff ignimbrite sheet has shown that this is not a tenable model for the Green Tuff ignimbrite. Unlike Taupo, the Green Tuff eruption did not have an initial ultraplinian column: pumice fall deposits are found only very locally and their thickness and grainsize decreases dramatically from source, indicating a low eruption column height (Williams 2010). The run-out distance was probably a function of mass flux (Bursik & Woods 1996; Branney & Kokelaar 1997; Branney & Kokelaar 2002; Roche et al., 2021), and as the mass flux changed, so did the run-out distance and ability to surmount topographic highs (Williams et al. 2014).

Williams et al., 2014 demonstrated that the Green Tuff was not deposited from a radially expanding density current and it did not immediately flow out to the distal limit of the ignimbrite sheet in all directions (c.f. e.g. Ui et al. 1989; Suzuki & Ui 1983; Dade 2003). Neither was it produced entirely by lateral shingling, nor did it arise as a result of sectoral flow whose orientation shifted clockwise (or anticlockwise) with time. Rather, the leading edge gradually advanced with time, progressively inundating the island as the current waxed, advancing with different rates in different sectors. Lateral shingling is observed locally where the footprint of the current laterally shifted with time, ultimately resulting in a broadly circular deposit (Williams et al. 2014). During periods of initial waxing and post-climactic waning, shifting flow was most pronounced, and strongly controlled by local topography which deflected the current. True radial flow was only achieved (barring the effect of the highest topographic obstacles) during times of peak flow (t4-6). In this period, the ignimbrite underwent progressive aggradation to form a layer-cake architecture, though inconsistently. When the current waned, the current became valley-confined and the leading edge of the current progressively retreated source-ward, at different rates in different sectors, despite flow continuing from source.

4.3 Flow bypassing

The inference of diachronous emplacement over a topographic barrier and progressive inundation of barriers has relied on detailed mapping and geochemical sampling. Most useful were samples collected from the base of the Green Tuff ignimbrite where a contact with the underlying unit was clearly seen. PDCs do not always deposit along their entire reach; some will involve broad bypass zones in which the current passes over land without leaving any deposit (e.g. Brown & Branney 2004). Therefore, we must consider how well the deposit footprint represents the full extent of the current. Whilst we cannot completely discount bypassing in the Green Tuff, we do not think it was significant for the following three reasons. Firstly, bypass zones often occur on steep slopes where the current is accumulative or uniform (Brown & Branney 2004). On Pantelleria, steep slopes are restricted to caldera walls, which are commonly draped by the Green Tuff Ignimbrite. Secondly, nowhere on Pantelleria are zones discovered distally where proximal equivalents are absent, such as is common where bypassing has been documented (e.g. Tenerife, Brown & Branney 2004). And finally, the peralkaline nature of the Green Tuff Ignimbrite means that the hot pyroclasts were very ‘sticky’ leading to near-instantaneous agglutination rather than post-depositional load welding (Mahood 1984; Branney et al., 2004). It is therefore unlikely in this case that the current was able to bypass without leaving a deposit. However, this would need to be considered if the method employed in this study was to be applied to other ignimbrites. If the current had been able to bypass without depositing, it is likely that the footprint areas would have been larger.

4.4 Evidence for caldera collapse

Two different calderas are proposed for the Green Tuff ignimbrite eruption: (1) The Monastero caldera (Cornette et al., 1983; Civetta et al., 1988; Orsi et al., 1991) and (2) the Cinque Denti caldera (Mahood & Hildreth, 1986). Along both the Monastero fault and the Piano Ghirlanda fault the entire Green Tuff Formation is cut by the fault scarp, indicating fault movement after emplacement of the Green Tuff (perhaps in late stages of the eruption). However, the north and eastern rims of possible calderas are unclear. The proposed Monastero Caldera is assumed to have buried, unidentified northern scarps whereas the proposed Cinque Denti caldera is thought to share its northern scarps with the La Vecchia caldera (La Vecchia caldera, age 106-175 ka; Mahood & Hildreth, 1986).

Two models can explain the stratigraphic relationships between the truncated and draping Green Tuff and the northern caldera walls revealed in this study. The first is that the caldera scarp did not exist until partway through Green Tuff ignimbrite deposition, then caldera collapse truncated the lowermost stratigraphy and then the draping part of the ignimbrite was deposited (chemical-entrachron zone t_2). The second scenario is that the scarp existed prior to the Green Tuff eruption, and the non-welded lowermost units of the Green Tuff ignimbrite either bypassed the c. 60° slope, were stripped off by succeeding parts of the current, or were reworked down the slope. Kinematic indicators observed in the densely welded units present on the inboard caldera scarps evidence both primary deposition of the lowermost part of the formation, where arriving pyroclasts were 'sticky' enough to agglutinate against the slope *and* rheomorphic slumping of the welded uppermost part of the formation. This suggests that the caldera wall existed prior to the formation of these deposits. The chemical composition of the draping parts of the ignimbrite implies that either the scarp was formed very early in the Green Tuff eruption (i.e. halfway through t_1 or t_2), or that the scarp already existed and that the loose and poorly welded lowermost parts of zone t_2 were not able to be deposited upon the steep slope (c. 60°). The early phases of the eruption are characterised by a weak sub-Plinian column evidenced by a limited pumice fall deposit. This is followed by a hybrid pyroclastic lithofacies interpreted to record hybrid fall and PDCs thought to record vent widening process leading to the initiation of PDC activity (Dowey and Williams, 2022). Given that the eruption during time-slices t_1 and t_2 appears to have been weak and sluggish, it seems unlikely that the caldera would have collapsed during these stages, at least not to the full extent suggested by the c. 200 m high scarps, though it does not discount minor movement along pre-existing faults. Therefore, there is not strong evidence that there was new caldera development or significant fault movement along the northern faults of the proposed Cinque Denti caldera of Mahood & Hildreth, 1986. Reactivation of these faults at depths now buried however, cannot be discounted nor can the possibility of buried scarps inboard of these faults (e.g. the proposed Monastero Caldera).

Lithic breccias are most developed along the Monastero caldera scarp, where the Green Tuff is clearly faulted and it does not drape the scarp. The best developed breccias in more distal sections of the Green Tuff also occur in this SW sector of the island. Therefore, it is possible that there was fault displacement along this scarp during the Green Tuff eruption. But the lithic breccias do not occur in the same time-slice at all locations. A lithic breccia commonly occurs in zone t_6 just as at the type locality however, lithic breccias also occur within zones t_3 to t_7. The lithic breccia is not found in the first phases of the eruption (t_1 or t_2), where one might be expected if a caldera-forming event caused the lower horizons (zone t_2) on the Kattibucale and Zinedi scarps to be faulted. If there was a caldera collapse during the Green Tuff eruption the diachronous nature of the lithic breccias suggests that movement along the faults may not have occurred during a distinct caldera-collapse phase. Instead, any collapse may have been progressive and incremental during the eruption. Far better developed, thick, coarse-grained lithic breccias are present in the pre-Green Tuff ignimbrites (Jordan et al., 2018; Rotolo et al., 2021) and probably record caldera collapse eruptions.

5 Conclusions

The Green Tuff Formation shows strong geochemical grading from pantellerite at the base to trachyte at the top and is represented at a type section located along the Monastero Caldera Scarp (Fig. 1). The Green Tuff is a deposit from a single eruption that has tapped a single, compositionally zoned magma chamber with the pantellerite and trachyte being the products of extreme crystal fractionation of a parental basalt (White et al. 2009; Neave et al. 2012).

The progressively aggraded ignimbrite records the chemical variations from the source, and a systematic decrease in Zr with height through the Green Tuff. The chemical variation has

been used to define a chemical ‘stratigraphy’ and can be interpreted as a proxy for time. Identifying the chemical characteristics of a section of the ignimbrite, anywhere across the island, has enabled placement of that location into the type section chemical stratigraphy. This information has allowed us to reconstruct the ignimbrite’s emplacement and interpret the current’s flow behavior.

The hypothesis that radially distributed ignimbrites are emplaced rapidly, simultaneously from source does not give the full picture. The Green Tuff Ignimbrite was emplaced diachronously while the PDC advanced over the island and then retreated again. Only during the climactic phases was the ignimbrite emplaced radially, though not uniformly. It is also shown that the leading edge of the current shifted laterally, as well as transversely, from vent. As the eruption waned, the leading edge of the current retreated despite the current still flowing from source. This is the first study of any kind to demonstrate that this has occurred.

Topography strongly affected the Green Tuff’s distribution. The initial leading edge of the current in its earliest phases did not surmount any of the studied topographic obstacles. Even small (c. 15 m high) barriers were sufficient to block, deflect or reflect the current, and the largest barriers were only inundated during the most climactic phase of the eruption. Thus, we have interpreted the initial stages of the current, t1 and t2, as likely to have been thin and low velocity. Topographic barriers were progressively inundated during waxing phases of the current as the mass flux and velocity of the current increased. Thin ignimbrite on valley sides does not always represent a stratigraphically condensed equivalent of the valley fill.

We infer that mass flux strongly controlled the current’s ability to scale topographic barriers and the radial extent over which the current flowed. This has important implications for estimates of velocity, volume, mass flux and run-out distances, which impact on the models that rely on these parameters to simulate PDCs.

The detailed study of the internal chemical-architecture of the single flow unit has elucidated important information on the dynamics of the eruption and the behavior of the PDC that deposited it. This complex internal architecture is cryptic and cannot be inferred from lithofacies variations. This technique could be easily applied to other compositionally zoned ignimbrites to further test the assumptions of their emplacement. Of particular interest would be other large, low-aspect ratio ignimbrites that can be traced distally from source, unlike the Green Tuff Formation which is constrained by its proximity to the sea. The chemical stratigraphy concept would be much more easily applied to unwelded ignimbrites, allowing for even closer spaced sampling, although these may not be as pristine, or be preserved on steep slopes.

References

Andrews, B. J., & Manga, M. (2011). Effects of topography on pyroclastic density current runout and formation of coignimbrites. *Geology*, *39*(12), 1099-1102.

Anastasakis, G. & Pe-Piper, G. 2006. An 18 m thick volcaniclastic interval in Pantelleria Trough, Sicily Channel, deposited from a large gravitative flow during the Green Tuff eruption. Marine Geology, 231, 201-219.

Andrews, G. D., & Branney, M. J. (2011). Emplacement and rheomorphic deformation of a large, lava-like rhyolitic ignimbrite: Grey's Landing, southern Idaho. *Bulletin*, *123*(3-4), 725-743.

Aramaki, S. & Ui, T. 1966. The Aira and Ata pyroclastic flows and related caldera and depressions in southern Kyushu, Japan. Bulletin of Volcanology, 29, 29-47.

Aravena, A., Roche, O. Influence of the topography of stratovolcanoes on the propagation and channelization of dense pyroclastic density currents analyzed through numerical simulations. *Bull Volcanol* **84**, 67 (2022). https://doi.org/10.1007/s00445-022-01576-2

Auker, M.R., Sparks, R.S.J., Siebert, L. *et al.* A statistical analysis of the global historical volcanic fatalities record. *J Appl. Volcanol.* **2**, 2 (2013). https://doi.org/10.1186/2191-5040-2-2

Barberi, F., Ghigliotti, M., Macedonio, G., Orellana, H., Pareschi, M. T. & Rosi, M. 1992. Volcanic Hazard Assessment of Guagua Pichincha (Ecuador) Based on Past Behavior and Numerical-Models. Journal of Volcanology and Geothermal Research, 49, 53-68.

Bourdier, J. L. & Abdurachman, E. K. 2001. Decoupling of small-volume pyroclastic flows and related hazards at Merapi volcano, Indonesia. Bulletin of Volcanology, 63, 309-325.

Brand, B. D., & Clarke, A. B. (2012). An unusually energetic basaltic phreatomagmatic eruption: using deposit characteristics to constrain dilute pyroclastic density current dynamics. *Journal of Volcanology and Geothermal Research*, *243*, 81-90.

Branney, M. J. & Kokelaar, P. 1992. A Reappraisal of Ignimbrite Emplacement - Progressive Aggradation and Changes from Particulate to Nonparticulate Flow during Emplacement of High-Grade Ignimbrite. Bulletin of Volcanology, 54, 504-520.

Branney, M. J. & Kokelaar, P. 1997. Giant bed from a sustained catastrophic density current flowing over topography: Acatlan ignimbrite, Mexico. Geology, 25, 115-118.

Branney, M. J. & Kokelaar, B. P. 2002. Pyroclastic density currents and the sedimentation of ignimbrites. Memoir / Geological Society of London ; no.27, 143.

Branney, M. J., Barry, T. L. & Godchaux, M. 2004. Sheathfolds in rheomorphic ignimbrites. Bulletin of Volcanology, 66, 485-491.

Brown, R. J. & Branney, M. 2004. Bypassing and diachronous deposition from density currents: Evidence from a giant regressive bed form in the Poris ignimbrite, Tenerife, Canary Islands. Geology, 32, 445-448.

Burgisser, A. 2005. Physical volcanology of the 2,050 BP caldera-forming eruption of Okmok volcano, Alaska. Bulletin of Volcanology, 67, 497-525.

Bursik, M. I. & Woods, A. W. 2000. The effects of topography on sedimentation from particle-laden turbulent density currents. Journal of Sedimentary Research, 70, 53-63.

Bursik, M. I. & Woods, A. W. 1996. The dynamics and thermodynamics of large ash flows. Bulletin of Volcanology, 58, 175-193.

Calder, E. S., Cole, P. D., Dade, W. B., Druitt, T. H., Hoblitt, R. P., Huppert, H. E., Ritchie, L., Sparks, R. S. J. & Young, S. R. 1999. Mobility of pyroclastic flows and surges at the Soufriere Hills Volcano, Montserrat. Geophysical Research Letters, 26, 537-540.

Capra, L., Sulpizio, R., Márquez-Ramirez, V. H., Coviello, V., Doronzo, D. M., Arambula-Mendoza, R., & Cruz, S. (2018). The anatomy of a pyroclastic density current: The 10 July 2015 event at Volcán de Colima (Mexico). *Bulletin of Volcanology*, **80**(4). **https://doi.org/10.1007/s00445-018-1206-4**

Catalano, S. G., G.; Lanzafame, G.; Tortorici, L. 2007. Fenomeni di reomorfismo nell'Ignimbrite Verdi di Pantelleria: strutture di flusso primario o secondario? Rendiconti Società Geologica Italiana, Nuova Serie, 4, 174-176.

Charbonnier, S. J., Garin, F., Rodríguez, L. A., Ayala, K., Cancel, S., Escobar-Wolf, R., ... & Calder, E. S. (2023). Unravelling the dynamics and hazards of the June 3rd, 2018, pyroclastic density currents at Fuego volcano (Guatemala). *Journal of Volcanology and Geothermal Research*, *436*, 107791.

Charbonnier, S. J., Germa, A., Connor, C. B., Gertisser, R., Preece, K., Komorowski, J. C., et al. (2013). Evaluation of the impact of the 2010 pyroclastic density currents at Merapi volcano from high-resolution satellite imagery, field investigations and numerical simulations. *Journal of Volcanology and Geothermal Research*, **261**, 295–315. https://doi.org/10.1016/j.jvolgeores.2012.12.021

Civetta, L., Cornette, Y., Gillot, P. Y. & Orsi, G. 1988. The Eruptive History of Pantelleria (Sicily Channel) in the Last 50 Ka. Bulletin of Volcanology, 50, 47-57.

Cornette, Y., Crisci, G. M., Gillot, P. Y. & Orsi, G. 1983. Recent volcanic history of pantelleria: A new interpretation. Journal of Volcanology and Geothermal Research, 17, 361-373.

Dade, W. B. (2003). The emplacement of low-aspect ratio ignimbrites by turbulent parent flows. *Journal of Geophysical Research: Solid Earth*, *108*(B4).

Dowey, N., & Williams, R. (2022). Simultaneous fall and flow during pyroclastic eruptions: A novel proximal hybrid facies. *Geology*, *50*(10), 1187-1191.

Edwards, D. A., Leeder, M. R., Best, J. L. & Pantin, H. M. 1994. On Experimental Reflected Density Currents and the Interpretation of Certain Turbidites. Sedimentology, 41, 437-461.

Ferriz, H. & Mahood, G. A. 1984. Eruption Rates and Compositional Trends at Los-Humeros-Volcanic-Center, Puebla, Mexico. Journal of Geophysical Research, 89, 8511-8524.

Fierstein, J. & Wilson, C. J. N. 2005. Assembling an ignimbrite: Compositionally defined eruptive packages in the 1912 Valley of Ten Thousand Smokes ignimbrite, Alaska. Geological Society of America Bulletin, 117, 1094-1107.

Fisher, R. V. 1990. Transport and Deposition of a Pyroclastic Surge across an Area of High Relief - the 18 May 1980 Eruption of Mount St-Helens, Washington. Geological Society of America Bulletin, 102, 1038-1054.

Fisher, R. V., Orsi, G., Ort, M. & Heiken, G. 1993. Mobility of a Large-Volume Pyroclastic Flow - Emplacement of the Campanian Ignimbrite, Italy. Journal of Volcanology and Geothermal Research, 56, 205-220.

Flynn, I. T. W., & Ramsey, M. S. (2020). Pyroclastic density current hazard assessment and modeling uncertainties for Fuego Volcano, Guatemala. *Remote Sensing*, **12**(17), 2790.

Fujii, T., & Nakada, S. (1999). The 15 September 1991 pyroclastic flows at Unzen Volcano (Japan): A flow model for associated ash-cloud surges. *Journal of Volcanology and Geothermal Research*, **89**(1–4), 159–172. https://doi.org/10.1016/S0377-0273(98)00130-9

Gardner, J. E., Burgisser, A. & Stelling, P. 2007. Eruption and deposition of the Fisher Tuff (Alaska): Evidence for the evolution of pyroclastic flows. Journal of Geology, 115, 417-435.

Giordano, G., De Rita, D., Cas, R. & Rodani, S. 2002. Valley pond and ignimbrite veneer deposits in the small-volume phreatomagmatic 'Peperino Albano' basic ignimbrite, Lago

Albano maar, Colli Albani volcano, Italy: influence of topography. Journal of Volcanology and Geothermal Research, 118, 131-144.

Jordan, N.J., Rotolo, S.G., Williams, R., Speranza, F., McIntosh, W.C., Branney, M.J., Scaillet, S., (2018). Explosive eruptive history of Pantelleria, Italy: repeated caldera collapse and ignimbrite formation at a peralkaline volcano, J. Volcanol. Geoth. Res., Volume 349 67-73

Kneller, B., Edwards, D., Mccaffrey, W. & Moore, R. 1991. Oblique Reflection of Turbidity Currents. Geology, 19, 250-252.

Kubo Hutchison, A., & Dufek, J. (2021). Generation of overspill pyroclastic density currents in sinuous channels. *Journal of Geophysical Research: Solid Earth*, *126*(10), e2021JB022442.

Legros, F. & Kelfoun, K. 2000. On the ability of pyroclastic flows to scale topographic obstacles. Journal of Volcanology and Geothermal Research, 98, 235-241.

Lirer, L., Petrosino, P. & Alberico, I. 2001. Hazard assessment at volcanic fields: the Campi Flegrei case history. Journal of Volcanology and Geothermal Research, 112, 53-73.

Macorps, E., Charbonnier, S. J., Varley, N. R., Capra, L., Atlas, Z., & Cabré, J. (2018). Stratigraphy, sedimentology and inferred flow dynamics from the July 2015 block-and-ash flow deposits at Volcán de Colima, Mexico. *Journal of Volcanology and Geothermal Research*, **349**, 99–116. **https://doi.org/10.1016/j.jvolgeores.2017.09.025**

Mahood, G. A. & Hildreth, W. 1986. Geology of the peralkaline volcano at Pantelleria, Strait of Sicily. Bulletin of Volcanology, 48, 143-172.

Miller, T. P. & Smith, R. L. 1977. Spectacular Mobility of Ash Flows around Aniakchak and Fisher Calderas, Alaska. Geology, 5, 173-176.

Neave, D. A., Fabbro, G., Herd, R. A., Petrone, C. M., & Edmonds, M. (2012). Melting, differentiation and degassing at the Pantelleria volcano, Italy. *Journal of Petrology*, *53*(3), 637-663.

Ogburn, S. E., & Calder, E. S. (2017). The relative effectiveness of empirical and physical models for simulating the dense undercurrent of pyroclastic flows under different emplacement conditions. *Frontiers in Earth science*, *5*, 83.

Ogburn, S. E., Calder, E. S., Cole, P. D., & Stinton, A. J. (2014). The effect of topography on ash-cloud surge generation and propagation. *Geological Society, London, Memoirs*, **39**(1), 179–194. **https://doi.org/10.1144/m39.10**

Ogburn, S.E., Charlton, D., Norgaard, D. *et al.* The Volcanic Hazard Maps Database: an initiative of the IAVCEI Commission on Volcanic Hazards and Risk. *J Appl. Volcanol.* **12**, 2 (2023). https://doi.org/10.1186/s13617-022-00128-9

Orsi, G., Ruvo, L. & Scarpati, C. 1991. The recent explosive volcanism at Pantelleria. Geologische Rundschau, 80, 187-200.

Pickering, K. T., Underwood, M. B. & Taira, A. 1992. Open-Ocean to Trench Turbidity-Current Flow in the Nankai Trough - Flow Collapse and Reflection. Geology, 20, 1099-1102.

Roche, O., Azzaoui, N., & Guillin, A. (2021). Discharge rate of explosive volcanic eruption controls runout distance of pyroclastic density currents. *Earth and Planetary Science Letters*, *568*, 117017.

Roche, O., Buesch, D. C., & Valentine, G. A. (2016). Slow-moving and far-travelled dense pyroclastic flows during the Peach Spring super-eruption. *Nature Communications*, *7*(1), 10890.

Saucedo, R., Macías, J., Bursik, M., Mora, J., Gavilanes, J., & Cortes, A. (2002). Emplacement of pyroclastic flows during the 1998–1999 eruption of Volcán de Colima, México. *Journal of Volcanology and Geothermal Research*, **117**(1–2), 129–153. **https://doi.org/10.1016/S0377-0273(02)00241-X**

Scarani, A., Faranda, C. F., Vona, A., Speranza, F., Giordano, G., Rotolo, S. G., & Romano, C. (2023). Timescale of emplacement and rheomorphism of the Green Tuff ignimbrite (Pantelleria, Italy). *Journal of Geophysical Research: Solid Earth*, *128*(7), e2022JB026257.

Schmincke, H. U. & Swanson, D. A. 1967. Laminar viscous flowage structures in ash-flow tuffs from Gran Canaria, Canary islands. Journal of Geology, 75, 641-664.

Sheridan, M. F. 1979. Emplacement of pyroclastic flows: A review. In: Chapin & Elston (eds.) Ash-flow tuffs. Geol. Soc. Am., Special Papers, 180, 125-136.

Sheridan, M. F., Stinton, A. J., Patra, A., Pitman, E. B., Bauer, A. & Nichita, C. C. 2005. Evaluating Titan2D mass-flow model using the 1963 Little Tahoma Peak avalanches, Mount Rainier, Washington. Journal of Volcanology and Geothermal Research, 139, 89-102.

Silvio G. Rotolo; Stéphane Scaillet; Fabio Speranza; John C. White; Rebecca Williams; Nina J. Jordan. Volcanological evolution of Pantelleria Island (Strait of Sicily) peralkaline volcano: a review. Comptes Rendus. Géoscience, Volume 353 (2021) no. S2, pp. 111-132. doi : 10.5802/crgeos.51. https://comptes-rendus.academie-sciences.fr/geoscience/articles/10.5802/crgeos.51/

Sulpizio, R., Capra, L., Sarocchi, D., Saucedo, R., Gavilanes-Ruiz, J. C., & Varley, N. R. (2010). Predicting the block-and-ash flow inundation areas at Volcán de Colima (Colima, Mexico) based on the present day (February 2010) status. *Journal of Volcanology and Geothermal Research*, **193**(1–2), 49–66. **https://doi.org/10.1016/j.jvolgeores.2010.03.007**

Suzuki, K. & Ui, T. 1983. Factors governing the flow lineation of a large-scale pyroclastic flow; an example in the Ata pyroclastic flow deposit, Japan. Bulletin Volcanologique, 46, 71-81.

Ui, T., Suzukikamata, K., Matsusue, R., Fujita, K., Metsugi, H. & Araki, M. 1989. Flow Behavior of Large-Scale Pyroclastic Flows - Evidence Obtained from Petrofabric Analysis. Bulletin of Volcanology, 51, 115-122.

Wang, R., Peakall, J., Hodgson, D. M., Keavney, E., Brown, H. C., & Keevil, G. M. (2025). Three-dimensional gravity current interactions with oblique slopes: Deflection, reflection and combined-flow behaviours. *Sedimentology*, *72*(7), 2121-2159.

White, J. C., Parker, D. F. & Ren, M. 2009. The origin of trachyte and pantellerite from Pantelleria, Italy: Insights from major element, trace element, and thermodynamic modelling. Journal of Volcanology and Geothermal Research, 179, 33-55.

Williams, R., (2010). Emplacement of Radial Pyroclastic Density Currents Over Irregular Topography: The Chemically-zoned, Low Aspect-ratio Green Tuff Ignimbrite, Pantelleria, Italy. University of Leicester, 10.6084/m9.figshare.789054.v1

Williams, R., Branney, M. J., & Barry, T. L. (2014). Temporal and spatial evolution of a waxing then waning catastrophic density current revealed by chemical mapping. *Geology*, *42*(2), 107-110.

Wilson, C. J. N. 1985. The Taupo Eruption, New-Zealand .2. The Taupo Ignimbrite. Philosophical Transactions of the Royal Society of London Series a-Mathematical Physical and Engineering Sciences, 314, 229.

Wilson, C. J. N., & Walker, G. P. L. (1981). Violence in pyroclastic flow eruptions. In *Tephra Studies: Proceedings of the NATO Advanced Study Institute" Tephra Studies as a Tool in Quaternary Research", held in Laugarvatn and Reykjavík, Iceland, June 18–29, 1980* (pp. 441-448). Dordrecht: Springer Netherlands.

Woods, A. W., Bursik, M. I. & Kurbatov, A. V. 1998. The interaction of ash flows with ridges. Bulletin of Volcanology, 60, 38-51.

Supplementary material

S 1 Geochemical Analysis Methodology

S 2 Green Tuff Formation lithofacies description and interpretation

S 3 Maps of the Green Tuff over topographic barriers